



## Review Article

# Thermal Aging of Menzolit BMC 3100

**Pavol Kostial,<sup>1</sup> Zora Kostialova Jancikova,<sup>1</sup> Ondrej Krejcar<sup>1,2</sup>, Kamil Kuca<sup>1,2</sup>,  
Oluwaseun Fadeyi,<sup>2,3</sup> Adebola Orogun,<sup>4</sup> and Robert Frischer<sup>1,2</sup>**

<sup>1</sup>VSB-Technical University of Ostrava, 17. Listopadu 15/2172, Ostrava 708 33, Czech Republic

<sup>2</sup>Center for Basic and Applied Research, Faculty of Informatics and Management, University of Hradec Kralove, Rokytanskeho 62, Hradec Kralove 500 03, Czech Republic

<sup>3</sup>Department of Geology, Faculty of Space and Environmental Science, University of Trier, Trier, Germany

<sup>4</sup>Adekunle Ajasin University, Akungba-Akoko, Nigeria

Correspondence should be addressed to Ondrej Krejcar; [ondrej.krejcar@uhk.cz](mailto:ondrej.krejcar@uhk.cz)

Received 8 July 2019; Accepted 9 March 2020; Published 8 May 2020

Academic Editor: Victor M. Castaño

Copyright © 2020 Pavol Kostial et al. This is an open access article distributed under the Creative Commons Attribution License, which permits unrestricted use, distribution, and reproduction in any medium, provided the original work is properly cited.

This paper deals with the influence of thermal aging on physical properties of a composite material, Menzolit BMC 3100. First, we present a number of analysis, FTIR (infrared spectroscopy), DSC (differential scanning calorimetry), TMA (thermomechanical analysis), TGA (thermogravimetric analysis), and HDT (heat deflection temperature), to understand the material performance under heat, and then, we carry out a test of toughness and strength using Charpy impact strength and Brinell hardness. Finally, we present optical surface analysis of the material under investigation by carrying out aging analysis at increments from room temperature up to 300°C. It was observed that above 200°C, the material begins to degrade at the surface, especially its organic component, polyester resin. This type of degradation has a negative impact on a variety of its physical properties. Exposure to temperatures above 200°C reduces the material's hardness, toughness, and shape stability, likewise, material degradation was found to increase with higher thermal loads almost linearly for all the observed properties.

## 1. Introduction

Menzolit BMC 3100 is a composite material that is sparsely described in the scientific literature. Detailed reference is only made to the material when producers give product specifications in offering the material as an advertised item. Such specifications are also limited, providing only specific physical values that characterise the material and rarely publishing details on material composition.

Polymer composites play very important roles in modern industry, especially the automotive sector [1–8], in which light weight, high specific modulus, and strength are critical factors put into consideration in production and where these materials find a wide range of application. This paper describes the composition of polymer composites, e.g., Menzolit BMC 3100, and the unique advantages they offer, relative to traditional materials. Details are given on prevailing market situation of polymer composites in Europe, and their special application in the European automotive

industry. Specific emphasis is also laid on the manufacturing of spare parts from thermoplastic, thermosetting plastics, and short and continuous fibre-reinforced composites. In [9–12], the authors offer insights on some recent technological and environmental applications of reinforced polymers. In [13], the author noted that Menzolit BMC 3100 is a special material developed for the automotive industry to produce headlights. This polymer composite material is gradually replacing traditional metal reflectors, mainly due to its simplicity and low cost in serial production. Nevertheless, future use of Menzolit BMC 3100 in modern automobile lighting systems pose an unanswered question, given the current use of “cold” light emitting diodes (LEDs) and laser for the same purpose and thermoplastic materials (e.g., polycarbonate) sufficing as heat resistant. Table 1 shows the properties of Menzolit BMC 3100 (given as average values of the test results) derived from nonpigmented, compression moulded panels at room temperature [13].

TABLE 1: Properties of Menzolit BMC 3100 (adapted from [13]).

Property	Value
Fibre content (%)	12
Moulding temperature (°C)	135–160
<sup>4</sup> Moulding pressure (bar)	20–80
Density (g/cm <sup>3</sup> )	2.0
<sup>1,3</sup> Shrinkage (%)	–0.03
<sup>3</sup> CTE (10 <sup>–6</sup> m/m·K)	10
HDT (°C)	>200
Glass transition temperature (°C)	185
<sup>2</sup> Continuous service temperature (°C)	190
<sup>3</sup> Young’s modulus (GPa)	14
<sup>3</sup> Tensile strength (MPa)	25
<sup>3</sup> Flex strength (MPa)	79
<sup>3</sup> Flex modulus (GPa)	11
<sup>3</sup> Impact strength (kJ/m <sup>2</sup> )	15
<sup>3</sup> Poisson’s ratio	0.30
Limited oxygen index (%)	22
<sup>5</sup> Glow wire (°C)	750
Fire retardancy 12 (level)	—
Volume resistivity (Ohm * cm)	10 <sup>15</sup>
Surface resistivity (Ohm)	10 <sup>12</sup>
Comparative tracking index (level)	CT1600
Water absorption (%)	<0.5

(1) negative values show expansion; (2) continuous service temperature without external loads; (3) if two figures are given for one property, the first refers to the transversal direction, while the second represents principal axis; (4) moulding pressure in compression moulding; (5) wall thickness 3 mm; (6) figures given apply to quasi-isotropic 6-layer [0/90/45/-45/90/0] design; (7) heat conductivity is understood perpendicular to the plane of the laminate (out-of-plane axis).

## 2. Theoretical Background

According to [14], composite producers provide a specific dataset useful for reference purpose, especially when designing these materials. Nevertheless, for best datasets, a number of experimental procedures may be necessary. One way is to determine a composite composition from the characteristics of its constituents.

While there seems to be extensive use of polymer matrix composites (particular the form reinforced with fibre) in aircraft structures [15] and automobile, accurate prediction of strength of the materials becomes very important [14, 16, 17]. The authors of studies such as [14] have researched how the reinforced forms of polymer matrix are impacted upon failure. Failure analysis is carried out on part of a composite material made up of polymeric matrix as well as fibre with the aim of understanding the stress-strain situation of the whole composite material (fibre and matrix included) [15]. This relationship is used to structurally predict matrix or fibre failure of the material. Depending on the kind of technique adopted, there is the possibility of individually predicting matrix failure and then fibre failure in a separate setup via computational methods [16, 17]. Nevertheless, advanced composite characteristics do not only depend on the kind of matrix, but the type of reinforcement also plays a vital role as well as a feature that is not associated to its composition, configuration of reinforcement. In some composite materials, only strengthening fibre concentration can be controlled, and composite dimensions

cannot be controlled [18]. A typical example is mouldable short fibre-reinforced thermoplastics. This paper thus offers a relatively comprehensive study of the physical parameters of BMC exposed to heat over a relatively large temperature range from ambient temperature to 300°C.

*2.1. Features of BMC 3100.* Menzolit BMC 3100 is typically designed using two unique kinds of moulding: compression moulding and injection moulding [13]. The former involves moulding Menzolit compounds using heat steel moulds with shear edges, as high density moulds generally offer the best results. Furthermore, 20–30 seconds-per-millimetre of wall thickness is preferred for curing when using compression mould. This is important as introduction of Menzolit compound to hot mould must be followed by a quick closing of the press to disallow precuring [13]. Injection moulding often takes place between 140°C and 165°C (standard compounds) and 30°C–40°C (injection unit). Back pressure is just needed to assure constant dosing, injection pressure varies between 50 and 250 bar, and injection time should be as short as possible but long enough to ensure ventilation. A small holding pressure should be applied until the gate is cured. A guide for curing is 10 seconds per millimetre of wall thickness [13].

*2.2. Thermoanalytical Techniques.* According to [19], thermal analysis refers to a number of heat measurement techniques in which physical properties of a substance are measured with respect to time or temperature while the temperature of the material, in a specified atmosphere, is either constantly heated or cooled (temperature programme) at a specific desired temperature. In [20], the author reported that thermoanalytical measurement generally depends on how temperature of a material interacts with volume, heat of reaction, and mass. These methods find a wide range of application in scientific discourse, ranging from pharmaceuticals [21], automobile, and aviation construction materials [22]. A number of thermoanalytical techniques exist in the literature. However, for the purpose of this study, only infrared spectrometry, differential scanning calorimetry, thermomechanical analysis, thermogravimetric analysis, and heat deflection temperature techniques are discussed. Differential scanning calorimetry, commonly abbreviated as DSC, deals with effects from physiochemical processes otherwise known as phase-transition reactions for which specific heat is a major constituent [23], so that heat flow rate into a substance is measured as a function of temperature while the temperature of the substance itself is programmed [24]. Via thermocouple, temperature difference (between sample and reference) is thus measured. Thermogravimetric analysis involves changes in mass as a result of material/substance interacting with the atmosphere, evaporation, and decomposition [23, 24]. It involves mass measurement of a material as a function of temperature, while subjecting the material to some form of controlled-temperature programmes. In [25], the author explained thermomechanical analysis as a measure of stiffness and damping properties of materials in terms of

temperature, time, and frequency, through the application of sinusoidal load to a specimen and subsequently measuring the resultant deformation. During this time, the sample undergoes controlled temperature programme. For heat deflection temperature, the polymer matrix of Menzolit BMC 3100 undergoes deformation, subject to a specified load. This temperature follows the ASTM D648 guidelines, with the test procedure similar to ISO 75 standards.

### 3. Method

Thermogravimetric analysis was carried out using a quantitative analysis of BMC composition with the aid of Hi-Res TGA TA Instruments 2950. Furthermore, isothermal analysis was used to determine the heat load time for up to 300 minutes. For degradation of the surface layer, the  $1147\text{ cm}^{-1}$  band corresponding to the C-O-C bond was closely monitored. Brinell hardness follows experimentally with the use of Brinell hardness tester ZWICK/ROELL.

### 4. Results and Discussion

A quantitative analysis of BMC composition (Figure 1) can be performed with thermogravimetric analysis (Hi-Res TGA TA Instruments 2950) [26, 27]. Depending on the weight-to-temperature ratio, data on the amount (mass) of the individual components in the sample can be obtained. For proper evaluation of the TGA curve, it is necessary to know the chemistry of ongoing decomposition reactions:

- 0–200°C: short-lived components up to 200°C; weight loss of the material's volatile components, especially styrene and moisture residues
- 200–600°C: decomposition of the polymeric, organic part of the material up to 600°C with dynamic heating of 20°C/min
- 600–800°C: decomposition of the  $\text{CaCO}_3$  filler
- 800°C: residue after combustion in air  $\text{CaO}$  + glass fibre

The resulting composition is as follows:

- 0.4% of short-lived components up to 200°C, representing mainly moisture content and residual styrene
- 20.6% of polymer matrix
- 63.6% of inorganic  $\text{CaCO}_3$  filler
- 15.4% of glass fibre

This is the percentage composition of the material of one batch of BMC. The composition may differ from one batch to another.

To determine the heat load time, an isothermal thermal analysis of a small amount of material was performed (up to 300 minutes). Figure 2 graphs the mass loss (in %) dependence on temperature. Mass loss increased above 240°C. Due to thermal degradation, the organic matrix decomposed in the surface layer. Decomposition is reflected by the loss of specific chemical bonds and the change in intensity of the

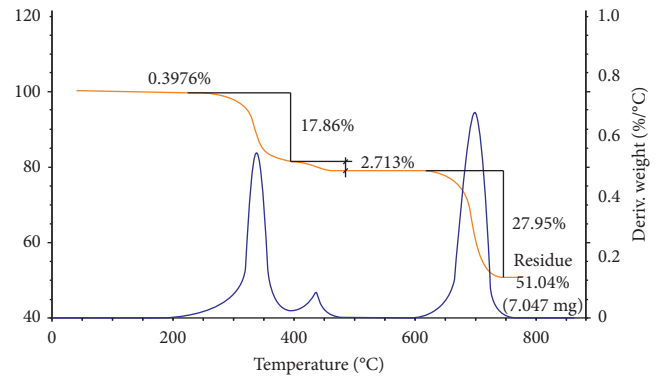


FIGURE 1: TGA decomposition curve of BMC.

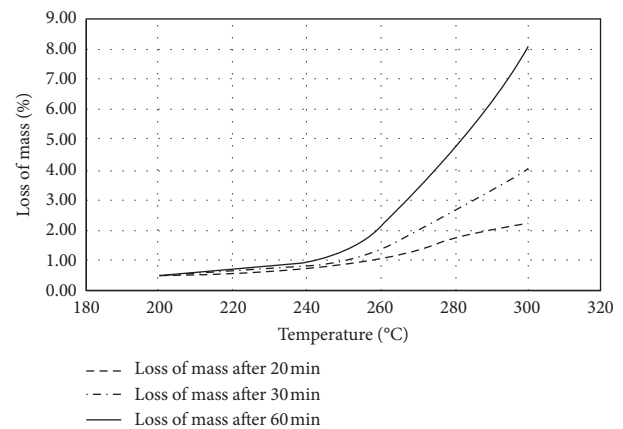


FIGURE 2: Mass loss dependence on temperature.

respective bands in the IR spectrum (FTIR Nicolet iS10 spectrophotometer).

The FTIR graph in Figure 3 shows the gradual decrease of bands corresponding to the bonds of the organic matrix of the polymer. To assess degradation of the surface layer, the  $1147\text{ cm}^{-1}$  band corresponding to the C-O-C bond was observed. With increasing temperature and progressive degradation of the surface layer, the polymeric matrix decomposed, resulting in a reduction in the intensity of the C-O-C bonding band. The  $1728\text{ cm}^{-1}$  band corresponds to the vibrational movement of the C=O bond, referred to as “stretching vibration” in acrylate groups of polyester resins, and the  $1147\text{ cm}^{-1}$  band corresponds to the stretching vibration of C-O-C bonds.

The results of surface decomposition are plotted in Figure 4. From the weight dependence of the load to the load temperature, the material was stable up to about 250°C with a heat load time of 30 minutes. This corresponds to the evaluation of FTIR surface analysis (see graph in Figure 4).

The next part of the experiment describes measurement of Brinell hardness (Brinell hardness tester ZWICK/ROELL). As the temperature increased, hardness was found to decrease (Figure 5). From 200°C, hardness decreased almost linearly. Conversely, the measurement time increased. Without heat stress, the bullet was crushed almost instantaneously. By contrast, after a 30-minute load at 300°C,

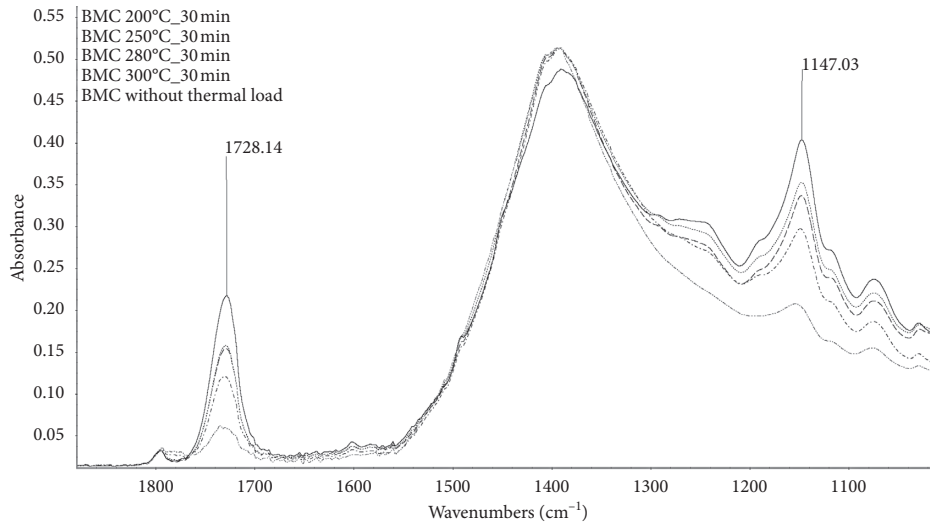


FIGURE 3: Details of binding zone C-O-C  $1147\text{ cm}^{-1}$ .

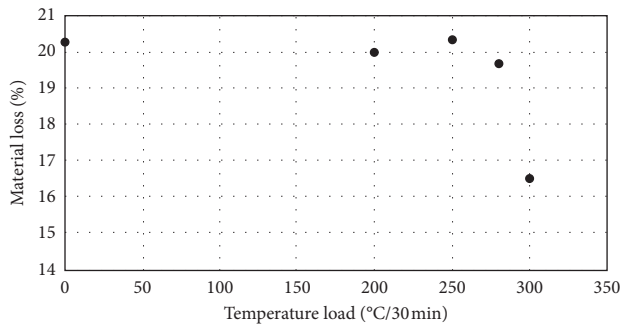


FIGURE 4: BMC material loss in relation to temperature load.

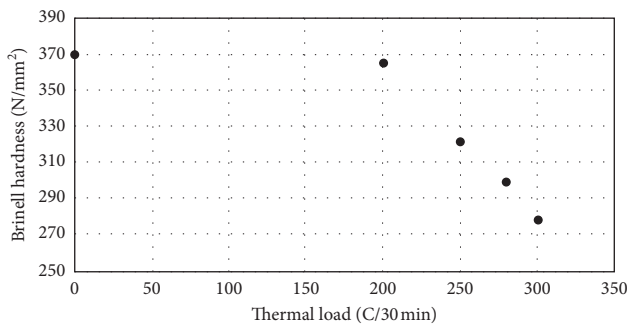


FIGURE 5: Brinell hardness dependence on thermal loading.

the specimen took a bullet for a while before the surface layer was pierced. As the temperature increased, it is likely that a “sintered” layer of material formed on the surface and that this material reduced the hardness of the material. Furthermore, the materials were tested for Charpy impact strength (CEAST Resil 5.5) versus loading temperature applied over 30 min. In this test, we also saw decreasing values with increasing temperature (Figure 6). The increase in impact strength at  $300^{\circ}\text{C}/30$  minutes could be due to the reinforcement/sintering of the sample surface. The results of the thermomechanical analysis (TMA TA Instruments 2940)

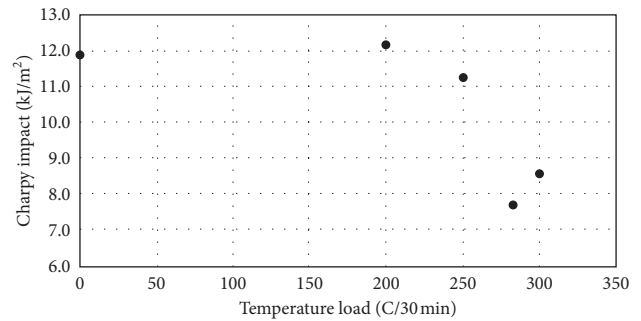


FIGURE 6: BMC-Charpy impact strength in relation to temperature load.

did not show any visible dependence on degradation (Figure 7). The only difference is visible between the unexposed sample, which had an additional cure reaction, and the most intensively loaded specimen at  $300^{\circ}\text{C}/30$  minutes, where the CLTE (linear thermal expansion coefficient) was almost linear over the entire temperature range.

Determining the glass transition temperature of BMC material with the DSC method (DSC Du Pont Instruments 2910) according to ISO 11357-2 was somewhat problematic. The material data sheet for BMC indicated a glass transition temperature ( $T_g$ ) of  $185^{\circ}\text{C}$  (according to ISO 11357-2). The determination method was set to meet the specified conditions. The signal response for BMC was very poor. No clearly identifiable transition (probably  $T_g$ ) was observed around  $185^{\circ}\text{C}$ . Certain transitions can be evaluated at around  $90^{\circ}\text{C}$  and  $130^{\circ}\text{C}$ . However, these were almost unidentifiable during the second heating, so it is possible that they may have been irreversible (temperature history, evaporation of volatile components, and absorbed moisture) (Figure 8). As the thermal load increased, the response diminished. The results were compared with the measured TA-Instruments thermoset curves [28]. The clear glass transition was not observable in any material, as the temperature range with the occurrence of glass transition always overlapped the cure reaction.

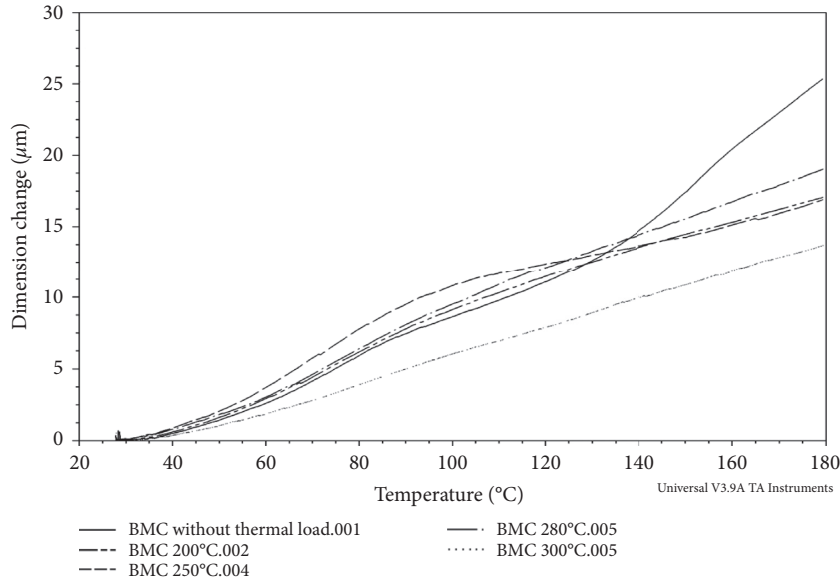


FIGURE 7: Thermal expansion curves for BMC depending on thermal load.

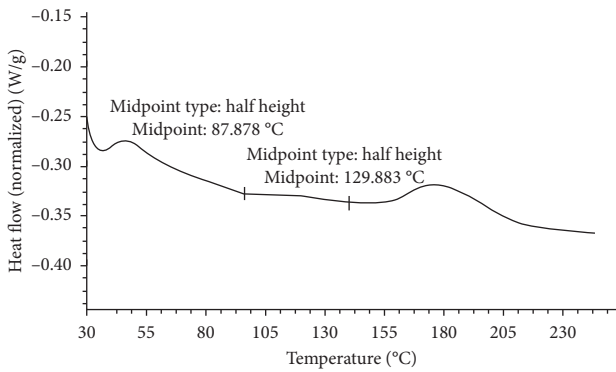


FIGURE 8: Sample without thermal load: 1<sup>st</sup> heating.

The weak signal response may have been due to the presence of a large percentage of inorganic fillers (limestone and glass fibre account for about 80% of the composite at the expense of the polymer matrix, which is only 20%). For this reason, heat is likely to be greatly diffused by the sample, and the reaction of the polymer matrix to increasing cell temperature was weak and the change in heat flow was not detectable.

During the first heating (1<sup>st</sup> step), the DSC curve showed undefined transitions around 90°C and 130°C. The transition stages were very small, so their interpretation is uncertain. The second heating (2<sup>nd</sup> step) did not show any changes in heat flow (Figure 9).

A noticeable change could be seen in the thermal history of the sample exposed to a heat load of 250°C on the DSC first heating curve (1<sup>st</sup> step). During the second heating (2<sup>nd</sup> step), these effects were no longer visible, and the DSC curve shows no significant heat flow changes (Figure 10).

The TMA dimension change curve reflects the DSC record of heat flow change [29]. Physical transitions caused nonlinearity of the stretch curve (Figure 11). The first

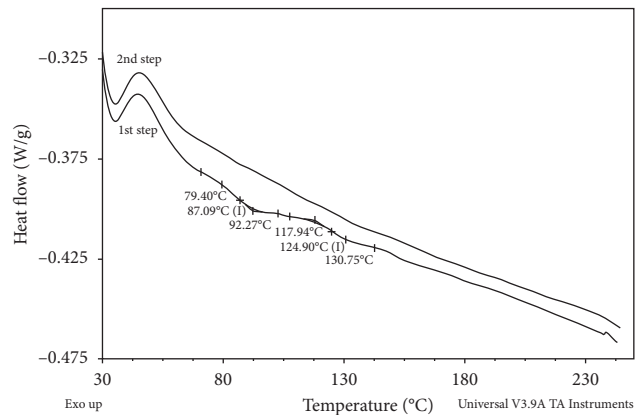


FIGURE 9: Sample after load 200°C/30 minutes: 1<sup>st</sup> heating (1<sup>st</sup> step); 2<sup>nd</sup> heating (2<sup>nd</sup> step).

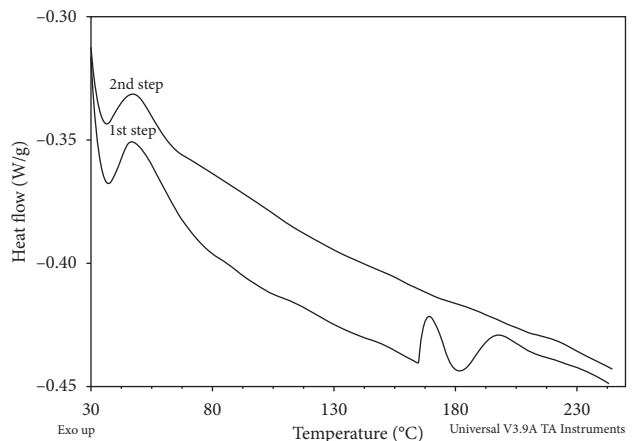


FIGURE 10: Sample after load 250°C/30 min: 1<sup>st</sup> heating (1<sup>st</sup> step); 2<sup>nd</sup> heating (2<sup>nd</sup> step).



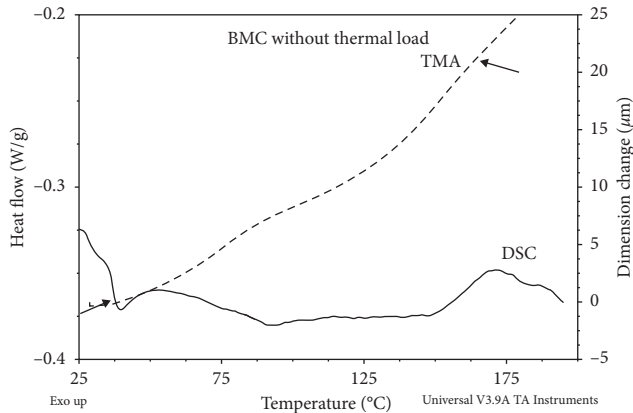


FIGURE 11: Comparison of DSC and TMA samples without heat exposure.

transition in the temperature range up to 100°C, corresponding to evaporating moisture and volatile components. At temperatures above 150°C, evidence of additional curing of the BMC on both curves is seen.

HDT (VICAT-HDT CEAST) measurement was based on ISO 75 for Plastics-Determination of deflection temperature under load. By default, a body of 10 mm thickness was used. The load was determined according to the standard at 0.45 or 1.82 MPa (method A or B). The resulting HDT temperature, according to the standard, indicated the temperature at which the test body had a deflection of 0.32 mm. As the BMC can withstand temperatures above 200°C, which is the maximum operating temperature of the HDT, the BMD had to be >200°C for all samples. The test was therefore designed to read deflection of the test body for the selected temperatures, and the dependence of shape deformation on rising temperature was plotted. Only the test conditions from the standard were used, which were a heating rate of 120°C/hr and a load of 1.82 MPa. From the results of the HDT test, it is clear that the sample deflection significantly increased with the applied heat load (Figure 12). Optical surface analysis showed the following results (KEYENCE digital 3D microscope). As we said above, Menzolit BMC 3100 belongs to the group “bulk moulding compounds” based on unsaturated polyester resin. The material is glass fibre reinforced. Figure 13 shows differently oriented glass fibres reaching about 500 µm in length and various CaCO<sub>3</sub> particles in the range of tens to hundreds of µm.

Figure 14 shows CaCO<sub>3</sub> particles in the range of tens to hundreds of µm. All are connected by a cross-linked polyester matrix. The filler structure is not preferentially oriented, but the fibres are randomly arranged or form the bonded bundles associated with the mineral filler and the resin. At a thermal load of 280°C/30 minutes, the surface layer of the material was visibly degraded to a depth of 60–70 µm. After thermal stress of 300°C/30 minutes, the surface layer was already damaged to a depth of about 90 µm. At a lower thermal load, degradation on the cross section was not so visible. This corresponds to the results of the TGA and FTIR analysis, where more degradation occurred at

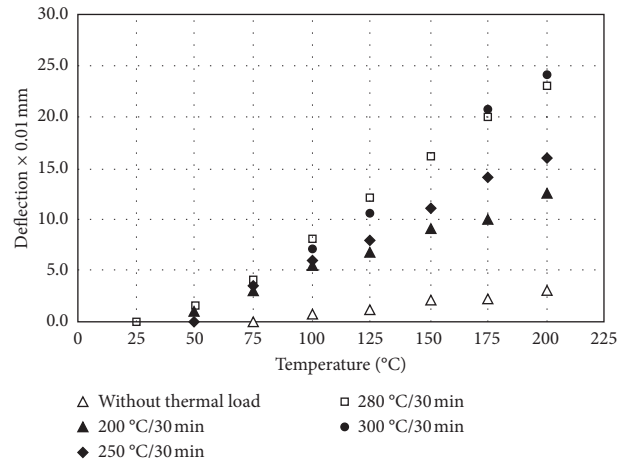


FIGURE 12: Determination of shape deflection (0.01 mm) plot according to temperature.

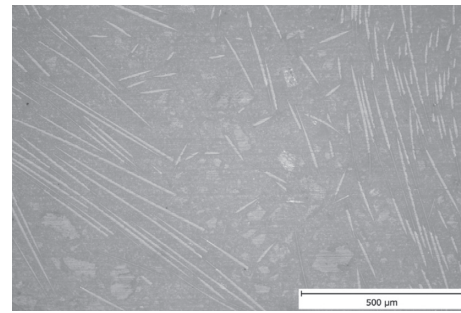


FIGURE 13: Differently oriented glass fibres.

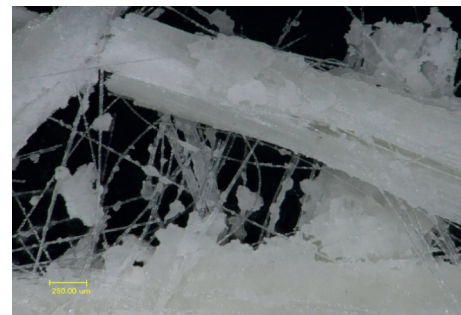


FIGURE 14: Randomly arranged fibres formed by bonded bundles associated with mineral filler and resin.

temperatures above 250°C. Only a colour change of the surface layer occurs below this temperature.

## 5. Limitations

Having critically examined the stability of Menzolit BMC 3100 under specific thermal conditions, the glass transition of the polymeric matrix could not be detected probably due to the large percentage of inorganic filler; therefore, it was not possible to study the effect of thermal degradation on its

value. Thermoanalytical techniques used in this study also have specific limitations for which each method may not be completely effective.

## 6. Conclusions

It is important to take note of the shape and quality of thermoanalytical curves so far discussed [30]. For example, for selected temperatures or mass losses as they have been interpreted in line with all demonstrated experimental conditions, consideration of the shapes and quality of the thermoanalytical curves helps to obtain further important information on Menzolit BMC 3100. The fundamentals of the techniques discussed and analysed in this study are functions of changes in the temperature profiles as a heat flux passes through a material [31], Menzolit 3100 in this case. Thermal techniques experimented tend to develop understanding of aging of the materials. Experimental results are therefore in comparison to the numerical simulations as functions of mass, weight, and temperature trends. The influence of thermal aging on physical properties of a composite material is detected experimentally for Menzolit BMC 3100, a composite material.

Menzolit BMC 3100 is a type of polycomponent composite material comprising an organic polymer matrix formed by polyester resin and two main inorganic components, a mineral filler of  $\text{CaCO}_3$  and irregularly arranged glass fibres. A suitable ratio of these components achieves a desired temperature resistance while maintaining sufficient mechanical properties for its intended use in the automotive industry.

Menzolit BMC 3100 can be considered a temperature-resistant composite material suitable for use in applications with continuous temperatures up to  $200^\circ\text{C}$ . Above this temperature, the material begins to degrade at the surface, especially its organic component (polyester resin). This type of degradation has a negative impact on a variety of its physical properties. Exposure to temperatures above  $200^\circ\text{C}$  reduces the material's hardness, toughness, and shape stability. Degradation increases with higher thermal loads almost linearly for all the observed properties.

## Conflicts of Interest

The authors declare that they have no conflicts of interest.

## Acknowledgments

This work was supported by the Ministry of Education, Youth and Sports, Czech Republic, in the framework of the project numbers SP2020/18, SP2020/61, and SP2020/39 at VSB Technical University of Ostrava, Czech Republic. The authors also acknowledge support of the project Smart Solutions in Ubiquitous Computing Environments, Grant Agency of Excellence, University of Hradec Kralove, Faculty of Informatics and Management, Czech Republic (ID: UHK-FIM-GE-2020).

## References

- [1] J. D. Ferry, *Viscoelastic Properties of Polymers*, Wiley, New York, NY, USA, 3rd edition, 1980.
- [2] J. E. Gordon, *The New Science of Strong Materials*, Princeton University Press, Princeton, NJ, USA, Paperback edition, 2018.
- [3] G. W. Ehrenstein, *Polymerní Kompozitní Materiály*, Scientia, Prague, Czech Republic, 2009.
- [4] H. F. Brinson and L. C. Brinson, *Polymer Engineering Science and Viscoelasticity: An Introduction*, Springer, New York, NY, USA, 2nd edition, 2014.
- [5] I. M. Ward and J. Sweeney, *Mechanical Properties of Solid Polymers*, Wiley, Chichester, UK, Third edition, 2012.
- [6] K. Friedrich and A. A. Almajid, "Manufacturing aspects of advanced polymer composites for automotive applications," *Applied Composite Materials*, vol. 20, no. 2, pp. 107–128, 2013.
- [7] S. W. Tsai and H. T. Hahn, *Introduction to Composite Materials*, Technomic Publishers, Westport, CT, USA, 1980.
- [8] W. Bobeth, "Fiber geometry," in *Textile Fibers: Texture and Properties*, W. Berger, H. Faulstich, and P. Fischer, Eds., pp. 89–116, Springer, Berlin, Germany, 1993.
- [9] A. Mirjalili, A. Zamanian, and S. M. M. Hadavi, "The effect of  $\text{TiO}_2$  nanotubes reinforcement on the mechanical properties and wear resistance of silica micro-filled dental composites," *Journal of Composite Materials*, vol. 53, no. 23, pp. 1–14, 2018.
- [10] A. Rafiq and N. Merah, "Nanoclay enhancement of flexural properties and water uptake resistance of glass fiber-reinforced epoxy composites at different temperatures," *Journal of Composite Materials*, vol. 53, no. 2, pp. 143–154, 2019.
- [11] S. Ivaturi, H. Baske, and P. Ghosal, "Distribution of milled carbon fibers as a function of their length on s-glass fabric and its effect on the electromagnetic properties of s-glass epoxy composites," *Journal of Composite Materials*, vol. 53, no. 20, pp. 2891–2899, 2018.
- [12] O. Rimmel, D. May, C. Goergen, A. Poeppel, and P. Mitschang, "Development and validation of recycled carbon fiber-based binder tapes for automated tape laying processes," *Journal of Composite Materials*, vol. 53, no. 23, pp. 3257–3268, 2019.
- [13] M. Menzolit, "The perfect composite for your demands," 2019.
- [14] V. Las, R. Zemčík, T. Kroupa, and R. Kottner, "Failure prediction of composite materials," *Bulletin of Applied Mechanics*, vol. 4, no. 14, pp. 81–87, 2008.
- [15] J. Wang and W. K. Chiu, "Prediction of matrix failure in fibre reinforced polymer composites," *Journal of Engineering*, vol. 2013, Article ID 973026, 9 pages, 2013.
- [16] J. Gosse and S. Christensen, "Strain invariant failure criteria for polymers in composite materials," in *Proceedings of the 19th AIAA Applied Aerodynamics Conference*, pp. 45–55, Anaheim, CA, USA, 2001.
- [17] D. L. Buchanan, J. H. Gosse, J. A. Wollschlager, A. Ritchey, and R. Byron Pipes, "Micromechanical enhancement of the macroscopic strain state for advanced composite materials," *Composites Science and Technology*, vol. 69, no. 11, pp. 1974–1978, 2009.
- [18] D. Schütz and J. J. Gerharz, "Fatigue strength of a fibre-reinforced material," *Composites*, vol. 8, no. 4, pp. 245–250, 1977.
- [19] D. Giron, "Applications of thermal analysis and coupled techniques in pharmaceutical industry," *Journal of Thermal Analysis and Calorimetry*, vol. 68, no. 2, pp. 335–357, 2002.
- [20] N. Soni, "Thermal methods of analysis," *Modern applications in Pharmacy & Pharmacology*, vol. 1, no. 2, 2017.

- [21] K. Alexander, P. Haines, and A. Riga, “Thermoanalytical instrumentation and applications,” in *Analytical Instrumentation Handbook*, J. Cazes, Ed., CRC Press, Boca Raton, FL, USA, Second edition, 2004.
- [22] F. Sedláček, V. Lašová, R. Kottner, and P. Bernardin, *Comparison of Numerical Simulation and Experiment of a Flexible Connecting Rod*, Industrial Engineering, Tallinn, Estonia, 2015.
- [23] M. E. Brown, *Introduction to Thermal Analysis: Techniques and Applications*, Kluwer Academic Publishers, New York, NY, USA, Second edition, 2001.
- [24] S. V. Cipriotti, M. Paciulli, and E. Chiavaro, “Application of different thermal analysis techniques to characterize oxidized olive oils,” *European Journal of Lipid Science and Technology*, vol. 119, no. 1, Article ID 1600074, 2017.
- [25] Linseis, *Thermomechanical Analysis—TMA Instruments of Linseis*, Linseis Messgeräte GmbH, Selb, Germany, 2015, <https://www.linseis.com/en/products/thermomechanical-analysis/>.
- [26] R. E. Wetton, “Thermomechanical methods,” in *Handbook of Thermal Analysis and Calorimetry*, M. E. Brown, Ed., Elsevier, Amsterdam, Netherlands, 1998.
- [27] V. S. Ramachandran, Ed., *Handbook of Thermal Analysis of Construction Materials*, William Andrew Publishing, Norwich, NY, USA, 2003.
- [28] M. Wagner, *Thermal Analysis in Practice: Fundamental Aspects*, Carl Hanser Verlag, Munich, Germany, 2017.
- [29] R. Häßler and W. Kunze, *Thermische Eigenschaften von Klebstoffen und Harzen: DMA—DSC—TGA—TMA; Stoffsammlung Thermoanalytischer Messkurven*, TA-Instruments, New Castle, DE, USA, 2010.
- [30] M. Feist, “Thermal analysis: basics, applications, and benefit,” *ChemTexts*, vol. 1, no. 1, p. 8, 2015.
- [31] S. Coutin, A. Chaves, and F. Just, “A thermal analysis approach for the detection of damage in carbon—carbon type composite,” *Journal of Composite Materials*, vol. 41, no. 12, 2007.